Doping-dependent nonlinear Meissner effect and spontaneous currents in high-T_c superconductors

Sheng-Chiang Lee, Mathew Sullivan, Gregory R. Ruchti,* and Steven M. Anlage
Center for Superconductivity Research, Department of Physics, University of Maryland, College Park, Maryland 20742-4111, USA

Benjamin S. Palmer
Laboratory for Physical Sciences, College Park, Maryland 20740, USA

B. Maiorov† and E. Osquiguil
Centro Atómico Bariloche and Instituto Balseiro, Comisión Nacional de Energía Atómica, 8400 S. C. de Bariloche, Río Negro, Argentina

(Received 20 May 2004; revised manuscript received 7 September 2004; published 11 January 2005)

We measure the local harmonic generation from superconducting thin films at microwave frequencies to investigate the intrinsic nonlinear Meissner effect near T_c in the zero magnetic field. Both second and third harmonic generation are measured to identify time-reversal symmetry breaking (TRSB) and time-reversal symmetric (TRS) nonlinearities. We perform a systematic doping-dependent study of the nonlinear response and find that the TRS characteristic nonlinearity current density scale follows the doping dependence of the depairing critical current density. We also extract a spontaneous TRSB characteristic current density scale that onsets at T_c, grows with decreasing temperature, and systematically decreases in magnitude (at fixed T/T_c) with underdoping. The origin of this current scale could be Josephson circulating currents or the spontaneous magnetization associated with a TRSB order parameter.

DOI: 10.1103/PhysRevB.71.014507 PACS number(s): 74.25.Nf, 74.25.Dw, 74.25.Sv, 74.78.Bz

It is predicted that all superconductors have an intrinsic nonlinear Meissner effect (NLME).[1–3] Many experiments have been conducted to observe this effect in high-T_c superconductors (HTSC).[4–8] Some of this work observed a linear-magnetic-field-dependent penetration depth at low temperature, in agreement with theory.[1,2] However, the quantitative, and some qualitative, details of the NLME signals in these experiments did not agree with the theory. This is most likely due to the presence of other, stronger, nonlinearities. In particular, most NLME experiments utilize sample geometries that induce large currents on poorly prepared and characterized edges and corners of the sample. This leads to extremely large edge currents, which can lead to vortex entry and nonlinear behavior that overwhelms the NLME.[9,10] Therefore, a measurement of the *local* nonlinear properties of superconducting samples without edge and corner effects involved is desired.

In addition, nonlinear mechanisms in superconductors are likely to be doping dependent. Experimental work[11,12] (including the one we present here) on doping-dependent third-order harmonics or intermodulation distortion in high-T_c cuprates suggest the time-reversal symmetric nonlinearities are doping dependent. On the other hand, time-reversal symmetry breaking nonlinearities are also expected to be doping dependent in these materials. For example, Varma[13] proposed a doping-dependent time-reversal symmetry breaking (TRSB) nonlinear mechanism, which involves microcurrents flowing along the bonds in the CuO_2 planes in all underdoped high-T_c superconductors for $T<T^*$ (the pseudogap temperature). An aspect of this proposal was tested by angular-resolved photoemission spectroscopy,[14,15] but no consensus on the results has been achieved. Therefore, an independent technique for detecting nonlinear mechanisms in superconductors is desired, and we believe that our near-field nonlinear microwave microscope is a suitable alternative.

We employ a near-field microwave microscope to produce currents at high spatial frequencies, allowing us to detect small domains (e.g., TRSB domain sizes are predicted to be $\sim 100\ \mu$m)[13] that may have distinct time-reversal symmetric (TRS) or TRSB nonlinearities. Measurements of the nonlinear properties of superconductors may give new insights into the basic physics of these materials.

The details of our microscope can be found elsewhere.[16–18] The basic idea is to send a microwave signal at frequency f to a local area of a superconducting film via the magnetic coupling between a loop probe and the sample surface, and to induce microwave currents in the sample far from the edges. The induced current distribution $J(x,y)$ is concentrated on a lateral length scale of $\sim 200\ \mu$m with maximum value $\sim 10^4$ A/cm^2, dictated by the geometry of the probe and its height (12.5 μm) above the sample surface. Since the sample is nonlinear, it generates higher harmonic currents at $2f$, $3f$, etc. in response to the driving microwave signal. Note that the $2f$ and $3f$ signals are spatially distributed as $J^2(x,y)$ and $J^3(x,y)$, respectively, and are more sharply peaked than the driving current distribution. This means that the nonlinear response comes from even a smaller area of the sample. The $2f$ signal implies the presence of TRSB nonlinearities, and $3f$ implies the presence of TRS nonlinearities, e.g. the NLME. These higher harmonic signals couple back to the microwave system, and are measured by a spectrum analyzer. The measurements are carried out inside a shielded environment consisting of two layers of mu metal (high permeability at room temperature), and two layers of cryo-perm (high permeability at low temperatures). The sample is supported by a nonmagnetic ultra-low-carbon

TABLE I. Summary of T_c, the finite transition width δT, and estimated hole concentration x of samples presented in this work.

Sample	T_c (K)	δT (K)	Hole concentration x
MCS48	~46	~3	0.082
MCS4	~54	~1.7	0.088
MCS50	~75	~1.3	0.116
MCS2	~84	~1.3	0.13
MCS3	~90	~0.7	0.16

steel base so that all measurements are carried out in a nominally zero static magnetic field (<1 μG).[17,18]

The harmonic generation is a very sensitive way to study superconducting nonlinearities. Harmonic measurements have been performed on superconducting films and crystals to study the microwave nonlinear behavior as a function of temperature and external magnetic field.[19–23] In addition, this method can be used to study the nonlinear response of specific superconducting structures, e.g. a superconducting bicrystal grain boundary.[16,18,24] In the present experiment, we use this technique to study the local nonlinear response of homogeneous superconductors as a function of doping.

Our samples are *c*-axis oriented $YBa_2Cu_3O_{7-\delta}$ (YBCO) thin films deposited on $SrTiO_3$ and $NdGaO_3$ substrates by pulsed laser deposition. The film thickness ranges from $t \sim 100$ to 200 nm. All samples were deposited as nearly optimally doped. After deposition, they were treated by reannealing in different oxygen pressures at different temperatures to achieve the desired doping levels.[25,26] Their transition temperatures were determined by measuring the ac susceptibility (in the two-coil transmission geometry at 120 kHz with magnetic fields ~1 mT) after the reannealing process. The hole concentration x is estimated using the measured T_c and the universal formula,[27] $T_c/T_c^{optimal}=1-82.6(x-0.16)^2$, where $T_c^{optimal}$ is taken as 93 K, the highest T_c we found from the literature. The summary of T_c and transition width δT of these samples along with the estimated hole concentration x is given in Table I.

The nonlinear response of superconductors is temperature dependent and much can be learned about the microscopic properties through measurement of the temperature dependence of $2f$ and $3f$ nonlinear signals (referred to as P_{2f} and P_{3f}). Shown in Fig. 1 is a typical $P_{2f}(T)$ and $P_{3f}(T)$ measured on an underdoped YBCO thin film. The ac susceptibility data show a sharp transition temperature at ~75 K. Both $P_{2f}(T)$ and $P_{3f}(T)$ show a peak near T_c. The peak in $P_{3f}(T)$ at $T \leqslant T_c$ is expected because the superfluid density is small and very sensitive to perturbations such as applied currents and magnetic fields.[3,28] The peak is well described by the NLME based on, e.g., the Ginzburg-Landau (GL) theory.[3,29] The inset to Fig. 1 shows a GL fit to the $P_{3f}(T)$ peak around T_c in nearly optimally-doped YBCO with $T_c \sim 89.9$ K. This fitting uses the quadratically current-dependent superfluid density derived in Ref. 3 for type II superconductors,

$$\frac{n_s(T,J)}{n_s(T,0)} = \frac{\lambda^2(T,0)}{\lambda^2(T,J)} \cong 1 - \frac{1}{2}\left(\frac{J}{J_0(T)}\right)^2,$$

where $J_0(T)=J_c(1-(T/T_c)^2)\sqrt{1-(T/T_c)^4}$ is the GL characteristic nonlinearity current scale, and J_c is the depairing critical current density at $T=0$. The superconductor is more sensitive to external perturbation (such as an applied current J) near T_c because $J_0(T)$ goes to zero there. A finite transition temperature width ΔT, cutoff screening length scale, and finite $J_0(T_c)$ are used to smear out the divergence of the nonlinear response in the fitting,[30] and the parameters for the shown curve are $T_c=89.9$ K, $\Delta T=0.45$ K, and $J_c \sim 10^{11}$ A/m^2.

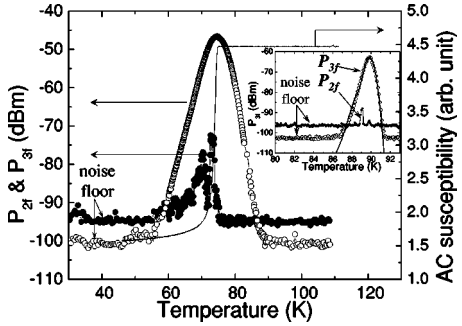

FIG. 1. A typical measurement of the second and third harmonic response versus temperature in an underdoped YBCO thin film. The open circles are the $P_{3f}(T)$ data, solid circles the $P_{2f}(T)$, and the solid line is the ac susceptibility data. Both P_{2f} and P_{3f} show a peak near T_c, and only P_{3f} extends to $T>T_c$. The inset is the harmonic measurement on an optimally doped YBCO fit to GL theory (solid line) with parameters $T_c=89.9$ K, finite transition width $\Delta T=0.45$ K, and $J_c \sim 10^{11}$ A/m^2.

However, we note that $P_{3f}(T)$ extends to temperatures substantially above T_c in the underdoped samples, which is not expected from the ordinary NLME. It may be due to the enhanced fluctuations in underdoped cuprates, which leads to the appearance of residual σ_2 at high frequencies above T_c.[31–33] The present work is focused on the doping dependence of the nonlinear response near T_c, and future work will examine the temperature dependence.

While the $P_{3f}(T)$ data are semiquantitatively understood (at least below T_c), the peak in $P_{2f}(T)$ is not expected from any theoretical proposals, to our knowledge. We performed a systematic study of $P_{2f}(T)$ and $P_{3f}(T)$ in underdoped YBCO thin films, and always observed this peak of $P_{2f}(T)$ near T_c, although it is smallest at optimal doping. Note that the experiment is performed inside four layers of magnetic shielding: two layers of mu metal and two of cryo-perm. This shielding reduces residual magnetic fields and we find that the $P_{2f}(T)$ and $P_{3f}(T)$ peaks are highly reproducible under these conditions.[17] Unlike the peak in $P_{3f}(T)$, $P_{2f}(T)$ does not extend to $T>T_c$, and abruptly onsets above the noise floor at $T_c(x)$ in all samples.

Both the magnitude and the width of the $P_{2f}(T)$ and $P_{3f}(T)$ peaks near T_c are systematically doping dependent. Figure 2 is a summary of $P_{2f}(T)$ and $P_{3f}(T)$ of differently doped YBCO thin films, with the temperature scaled by $T_c(x)$. A general trend of enhanced P_{2f} and P_{3f} near T_c, and broader distribution of $P_{2f}(T/T_c)$ and $P_{3f}(T/T_c)$ in the more underdoped YBCO is observed.

To quantitatively understand the doping dependence of nonlinearities from the harmonic data, we need to turn our data into a detail-independent measure that directly reflects the nonlinear mechanisms. It is generally accepted that the

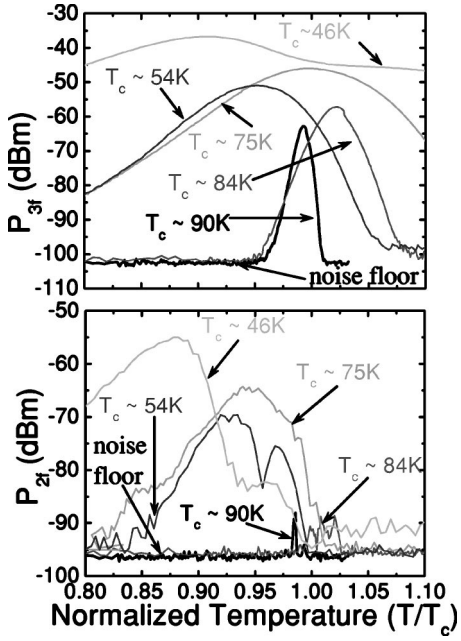

FIG. 2. A summary of $P_{2f}(T)$ and $P_{3f}(T)$ data measured from variously doped YBCO thin films. The temeprature is normalized by the T_c determined by ac susceptibility. The measured transition widths in ac susceptibility of these samples are shown in Table I.

current-dependent super-fluid density for the NLME can be generalized to describe the nonlinear behavior of other time-reversal symmetric (TRS) mechanisms as[34,35]

$$\frac{n_s(T,J)}{n_s(T,0)} = \frac{\lambda^2(T,0)}{\lambda^2(T,J)} \cong 1 - \left(\frac{J}{J_{\mathrm{NL}}(T)}\right)^2,$$

where n_s is the superfluid density, λ is the magnetic penetration depth, and J_{NL} is the nonlinear scaling current density, which depends on the nonlinear mechanisms (e.g., the depairing critical current density for the NLME). The expansion holds when $J/J_{\mathrm{NL}}(T) \ll 1$. The scaling current density quantitatively determines the degree of nonlinearity of the associated mechanism. The smaller the value of J_{NL}, the more nonlinear the associated mechanism.

Since the electromagnetic response of a superconductor is primarily inductive in nature, it is reasonable to assume that the reactance of a superconductor dominates its nonlinear response. Following an algorithm described in detail elsewhere,[16–18,35] we calculate the current-dependent superconducting inductance $L = L_0 + L_2 I^2$, and the third harmonic response generated by L_2. The power, P_{3f}, is proportional to the square of the third harmonic voltage developed on this nonlinear inductor, and depends on the penetration depth, applied power (P_f), frequency, $J_{\mathrm{NL}}(T)$, and the geometry of the driving current distribution $J(x,y)$. With this, we can extract the scaling current density from the $P_{3f}(T)$ data as,[16–18] $J_{\mathrm{NL}}(T,x) \cong \sqrt{11.94\Gamma \times \omega\mu_0\lambda^2(T,x)/4t^3\sqrt{2Z_0 P_{3f,measured}(T,x)}}$, where Γ is the geometry- and probe-dependent figure of merit of the microscope, $\Gamma \sim 31\ \mathrm{A}^3/\mathrm{m}^2$ at +12 dB m input microwave power, $\omega/2\pi \sim 6.5$ GHz is the driving frequency,

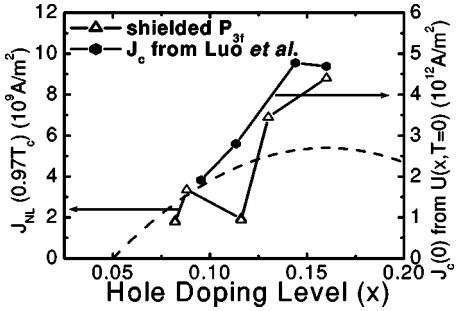

FIG. 3. A plot of $J_{\mathrm{NL}}(T=0.97T_c)$ extracted from P_{3f} data in Fig. 2 vs the doping level. The doping levels are estimated from T_c using the universal formula mentioned in the text and are summarized in Table I. The depairing critical current density at zero temperature J_c ($T=0$) extracted from the zero-temperature condensation energy by Luo *et al.* (Ref. 41) is plotted for a comparison. The dashed line schematically illustrates the superconducting dome in the phase diagram.

$Z_0 = 50\ \Omega$ is the characteristic impedance of coaxial transmission lines, t is the film thickness, and the numerical factor accounts for calibrated system-specific details (amplification, cable attenuation, etc.). Since the penetration depth λ is involved in the algorithm, to extract the doping-dependence of J_{NL} from experimental harmonic data we must consider the doping-dependent penetration depth [$\lambda(T,x)$ data are taken from the literature].[36–39]

Shown in Fig. 3 is the J_{NL} extracted from the $P_{3f}(T)$ data shown in Fig. 2 at a temperature of $0.97T_c$.[40] A trend of decreasing J_{NL} in the more underdoped YBCO films is observed. If the dominant nonlinear mechanism that gives rise to the P_{3f} signal near T_c is the NLME, then the extracted J_{NL} should be a measure of the depairing critical current density, J_c.

The depairing critical current density J_c is related to the thermodynamic critical field H_c, and the condensation energy density U of the superconductor as $J_c(T,x) \approx H_c(T,x)/\lambda(T,x) = \sqrt{2U(T,x)/\mu_0}/\lambda(T,x)$. Taking the doping-dependent penetration depth into account, the observed doping dependent J_{NL} implies that the condensation energy is also doping dependent. This statement is supported by the work of Luo *et al.*[41] who measured the doping-dependent zero-temperature condensation energy density $U(0,x)$ of YBCO ceramics. We extract $J_c(T=0)$ from their data and plot with our doping-dependent J_{NL} in Fig. 3 for comparison, where the doping trends are in good agreement.[42] This suggests that we have measured the doping dependence of the NLME nonlinear scaling current density in YBCO.

The observation of a P_{2f} signal near T_c implies the presence of TRSB nonlinearities and a spontaneously flowing current in or on the superconductor. To obtain a quantitative understanding of the measured P_{2f} signals, we phenomenologically propose that the spontaneous current simply modifies the NLME in a way leading to broken time-reversal symmetry:

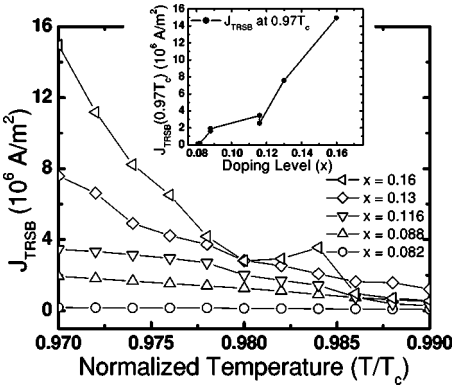

FIG. 4. The main figure is $J_{TRSB}(T/T_c)$ extracted from harmonic measurements of variously doped YBCO films. The temperature is normalized by T_c measured by ac susceptibility. The inset is a plot of $J_{TRSB}(T=0.97T_c)$ vs the doping level to show the doping dependence of J_{TRSB}.

$$\frac{n_s(T,J)}{n_s(T,0)} = \frac{\lambda^2(T,J)}{\lambda^2(T,0)} \cong 1 - \left(\frac{J - J_{TRSB}(T)}{J_{\mathrm{NL}}(T)}\right)^2 \cong 1 + \frac{2JJ_{TRSB}(T)}{{J_{\mathrm{NL}}}^2(T)} - \left(\frac{J}{J_{\mathrm{NL}}(T)}\right)^2,$$

where J_{TRSB} is the phenomenological spontaneous current density. Rewriting the linear term as $J/J_{\mathrm{NL}}{}'$, where $J_{\mathrm{NL}}{}' \equiv {J_{\mathrm{NL}}}^2/2J_{TRSB}$, we can follow a similar analysis algorithm[16–18,35] to extract $J_{\mathrm{NL}}{}'$; hence J_{TRSB}. As a result, we find that J_{TRSB} *can be extracted directly from the data* without considering the doping dependence of λ, or the precise value of T_c as

$$J_{TRSB}(T) \cong \frac{2.8(\mathrm{A/m})}{t}\sqrt{\frac{P_{2f,measured}(T)}{P_{3f,measured}(T)}}.$$

The extracted $J_{TRSB}(T)$ of YBCO films at different doping levels are shown in Fig. 4. Note that the data can only be presented in a temperature range where both P_{2f} and P_{3f} signals are above the noise floor, i.e., $0.97 < T/T_c < 0.99$. There are two trends observed in this figure. First is that $J_{TRSB}(T)$ of all underdoped YBCO films appears to onset at T_c, which can also be concluded from the $P_{2f}(T)$ data in Fig. 2. From the temperature-dependent J_{TRSB} shown in Fig. 4, it is likely that there is no J_{TRSB} above T_c, in striking contrast with the third harmonic (TRS) response. Second, the magnitude of J_{TRSB} at a fixed T/T_c generally decreases in the more underdoped films. To understand these behaviors, we must identify the origin of the nonlinear mechanism.

One possible mechanism for TRSB nonlinearities is Josephson vortices in a superconducting weak-link network. It is known that high-T_c cuprates, and particularly underdoped YBCO,[26] are often granular in nature. Although it is proposed that the superconducting order parameter onsets at much higher temperatures (pseudogap temperature) in underdoped cuprates, the long-range phase coherence is not established until the temperature reaches $T_c < T^*$.[43] This is a necessary condition for the existence of Josephson vortices in the weak-link network since long-range superconducting currents are required to circulate among the network.

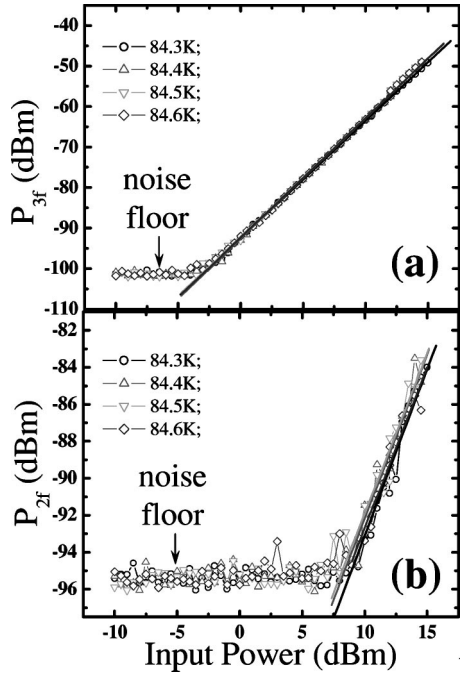

FIG. 5. The power-dependent (a) P_{3f} and (b) P_{2f} measured for the YBCO thin film with $x=0.13$ and fit at temperatures near $T_c \sim 84$ K. All axes are on a logarithmic scale. The solid lines are power-law fits with slopes of close to 3 and 2 for P_{3f} and P_{2f}, respectively, which is consistent with assumptions used in the algorithms for extracting J_{NL} and J_{TRSB} discussed in the text.

This argument suggests that the magnitude of J_{TRSB} ($\ll J_{\mathrm{NL}}$ at the same T/T_c) is on the order of the Josephson critical current density (10^7 A/m^2 at $T/T_c=0.97$) of the weak-link network. On the other hand, the doping dependence of J_{TRSB} implies that the Josephson critical current density is doping dependent. This statement is supported by the work of Sydow *et al.*,[44] who measured the Josephson critical current of 23° YBCO bicrystal grain boundaries at different doping levels. They found that the critical current drops by a factor of ~100 from an optimally doped junction to an underdoped junction of $T_c \sim 50$ K. We expect that the low-angle grain boundaries, which may be present in our films, demonstrate a similar doping dependence.

However, power-dependent measurements of P_{2f} near T_c are not entirely consistent with a Josephson vortex mechanism for P_{2f}. We observe a monotonic and uniform power-law dependence of $P_{2f}(P_f) \sim P_f^{1.8}$, as shown in Fig. 5. This is not expected from a Josephson nonlinearity, which should reveal a nonmonotonic power dependence of $P_{2f}(P_f)$, followed by saturation, as we have observed with the same microscope in an isolated YBCO bicrystal grain boundary,[16] and which is also expected from simulations.[45] The uniformity of the $P_{2f}(P_f)$ response suggests that a global nonlinear mechanism may be responsible for the observed signal.

The power dependence of P_{2f} is consistent with another possible mechanism for J_{TRSB}, namely the presence of an exotic TRSB order parameter associated with a temperature-dependent spontaneous magnetization.[13,46] This order param-

eter is expected to have a spontaneous magnetic field and current associated with it when translational symmetry is also broken.[47] Several possibilities for microscopic TRSB surface states in YBCO include $s+id_{x^2-y^2}$ and $d_{x^2-y^2}+id_{xy}$ wave pairing states, which may break into domains of degenerate states.[46] We note that the behavior of $J_{TRSB}(T)$ in Fig. 4 resembles that of a TRSB order parameter, such as that seen as an internal magnetic field in Sr_2RuO_4[48] by muon spin relaxation (μ-SR), for example. This suggests the possibility of a TRSB order parameter onset at T_c in underdoped cuprates. Also, several theorists have pointed out that an observation of fractional vortices with flux other than an integer or half-integer flux quanta would be an indication of broken time-reversal symmetry.[46,49] The experimental work of Tafuri and Kirtley[50] observed fractional vortices in *c*-axis YBCO films by scanning SQUID microscopy, consistent with this picture. They reported the enhancement of the local magnetization associated with these vortices as the temperature is decreased, consistent with our observation of larger J_{TRSB} at lower temperatures.

Note that the smallest measured magnetic field associated with J_{TRSB} can be estimated as $B \cong \mu_0 J_{TRSB} t \leqslant 0.1$ mG, where $t \sim 1000$ Å $< \lambda$ is the film thickness and $J_{TRSB} \sim 10^5$ A/m^2 is the smallest J_{TRSB} we measured. Note that the sensitivity limit to the local magnetic field claimed by μ-SR is about 100 mG.[48] This suggests that our microscope has excellent sensitivity to TRSB mechanisms in surface states and thin films. We also note that our microscope generates nonlinearity-induced current distributions on the length scale of at least one set of proposed TRSB domains.[13]

In conclusion, we have demonstrated direct measurements of the NLME near T_c of YBCO films at different doping levels, and found the depairing critical current density to decrease with the doping level below optimal. This is the first measurement of the doping dependence of the NLME, to our knowledge. We also observe a temperature- and doping-dependent TRSB nonlinearity from P_{2f} and P_{3f} measurements, which may be due to the presence of Josephson vortices in a weak-link network, or to the presence of a TRSB order parameter associated with domains of spontaneous magnetization. We phenomenologically introduce a spontaneous current J_{TRSB} to quantify the strength and doping dependence of this nonlinearity. Our results are free of edge effects, and have shown the unique ability of our technique to study weak local nonlinearities of superconductors.

We thank Juergen Halbritter for useful discussions. This work was supported by NSF/GOALI DMR-0201261, and the Microwave Microscope Shared Experimental Facility of the NSF/Maryland MRSEC DMR-0080008.

*Present address: Physics and Astronomy Department, Johns Hopkins University, Baltimore, Maryland 21218, USA.

†Present address: Superconductivity Technology Center, Mail Stop K763, Los Alamos National Laboratory, Los Alamos, New Mexico 87545, USA.

[1] S. K. Yip and J. A. Sauls, Phys. Rev. Lett. **69**, 2264 (1992).

[2] D. Xu, S. K. Yip, and J. A. Sauls, Phys. Rev. B **51**, 16 233 (1995).

[3] J. Gittleman, B. Rosenblum, T. E. Seidel, and A. W. Wicklund, Phys. Rev. **137**, A527 (1965).

[4] J. Buan, B. P. Stojkovic, N. E. Israeloff, A. M. Goldman, C. C. Huang, O. T. Valls, J. Z. Liu, and R. Shelton, Phys. Rev. Lett. **72**, 2632 (1994).

[5] A. Maeda, Y. Iino, T. Hanaguri, N. Motohira, K. Kishio, and T. Fukase, Phys. Rev. Lett. **74**, 1202 (1995).

[6] A. Carrington, R. W. Giannetta, J. T. Kim, and J. Giapintzakis, Phys. Rev. B **59**, R14 173 (1999).

[7] C. P. Bidinosti, W. N. Hardy, D. A. Bonn, and R. Liang, Phys. Rev. Lett. **83**, 3277 (1999).

[8] G. Benz, S. Wünsch, T. A. Scherer, M. Neuhaus, and W. Jutzi, Physica C **356**, 122 (2001).

[9] M. Hein, *High-Temperature Superconductor Thin Films at Microwave Frequencies* (Springer-Verlag, New York, 1999), Vol. 155.

[10] A. P. Zhuravel, A. V. Ustinov, K. S. Harshavardhan, and S. M. Anlage, Appl. Phys. Lett. **81**, 4979 (2002).

[11] D. E. Oates, S.-H. Park, M. A. Hein, P. J. Hirst, and R. G. Humphreys, IEEE Trans. Appl. Supercond. **13**, 311 (2003).

[12] M. A. Hein, R. G. Humphreys, P. J. Hirst, S. H. Park, and D. E. Oates, J. Supercond. **16**, 895 (2003).

[13] C. M. Varma, Phys. Rev. B **61**, R3804 (2000); M. E. Simon and C. M. Varma, *ibid.* **67**, 054511 (2003).

[14] A. Kaminski, S. Rosenkranz, H. M. Fretwell, J. C. Campuzano, Z. Li, H. Raffy, W. G. Cullen, H. You, C. G. Olson, C. M. Varma, and H. Höchst, Nature (London) **416**, 610 (2002).

[15] S. V. Borisenko, A. A. Kordyuk, A. Koitzsch, T. K. Kim, K. Nenkov, M. Knupfer, J. Fink, C. Grazioli, S. Turchini, and H. Berger, Phys. Rev. Lett. **92**, 207001 (2004).

[16] S.-C. Lee and S. M. Anlage, Appl. Phys. Lett. **82**, 1893 (2003); S.-C. Lee and S. M. Anlage, IEEE Trans. Appl. Supercond. **13**, 3594 (2003).

[17] S.-C. Lee, Ph.D. dissertation, University of Maryland, 2004.

[18] S.-C. Lee, S.-Y. Lee, and S. M. Anlage, Phys. Rev. B (to be published); cond-mat/0408170.

[19] C. Wilker, Z.-Y. Shen, P. Pang, W. L. Holstein, and D. W. Face, IEEE Trans. Appl. Supercond. **5**, 1665 (1995).

[20] A. Agliolo Gallitto and M. Li Vigni, Physica C **305**, 75 (1998).

[21] Balam A. Willemsen, K. E. Kihlstrom, T. Dahm, D. J. Scalapino, B. Gowe, D. A. Bonn, and W. N. Hardy, Phys. Rev. B **58**, 6650 (1998).

[22] J. C. Booth, L. R. Vale, and R. H. Ono, IEEE Trans. Appl. Supercond. **11**, 1387 (2001).

[23] E. E. Pestov, Y. N. Nozdrin, and V. V. Kurin, IEEE Trans. Appl. Supercond. **11**, 131 (2001).

[24] D. E. Oates, Y. M. Habib, C. J. Lehner, L. R. Vale, R. H. Ono, G. Dresselhaus, and M. S. Dresselhaus, IEEE Trans. Appl. Supercond. **9**, 2446 (1999).

[25] E. Osquiguil, M. Maenhoudt, B. Wuyts, and Y. Bruynseraede, Appl. Phys. Lett. **60**, 1627 (1992).

[26] B. S. Palmer, H. D. Drew, R. A. Hughes, and J. S. Preston, Phys. Rev. B **70**, 184511 (2004).

[27] J. L. Tallon, C. Bernhard, H. Shaked, R. L. Hitterman, and J. D. Jorgensen, Phys. Rev. B **51**, 12 911 (1995).
[28] G. Hampel, B. Batlogg, K. Krishana, N. P. Ong, W. Prusseit, H. Kinder, and A. C. Anderson, Appl. Phys. Lett. **71**, 3904 (1997).
[29] Note that the possible dielectric nonlinearities of the substrate do not contribute to the harmonic response measured here. See Ref. 16.
[30] The rough physical justifications for the GL fit parameters are as follows. The cutoff length scale $\lambda_{cut}=1.8\ \mu$m represents the transition to normal metal screening with a finite skin depth, and the non-zero value of $J_0(T_c)=3\times10^4\ \mathrm{A/cm^2}$ represents the finite superfluid response at T_c due to fluctuations.
[31] J. R. Waldram, D. M. Broun, D. C. Morgan, R. Ormeno, and A. Porch, Phys. Rev. B **59**, 1528 (1999).
[32] J. Corson, R. Mallozzi, J. Orenstein, J. N. Eckstein, and I. Bozovic, Nature (London) **398**, 221 (1999).
[33] C. Kusko, Z. Zhai, N. Hakim, R. S. Markiewicz, S. Sridhar, D. Colson, V. Viallet-Guillen, A. Forget, Yu. A. Nefyodov, M. R. Trunin, N. N. Kolesniov, A. Maignan, A. Daignere, and A. Erb, Phys. Rev. B **65**, 132501 (2002).
[34] T. Dahm and D. J. Scalapino, J. Appl. Phys. **81**, 2002 (1997).
[35] J. C. Booth, J. A. Beall, D. A. Rudman, L. R. Vale, and R. H. Ono, J. Appl. Phys. **86**, 1020 (1999).
[36] Y. S. Gou, H. K. Zeng, J. Y. Juang, J. Y. Lin, K. H. Wu, T. M. Uen, and H. C. Li, Physica C **364–365**, 408 (2001).
[37] D. A. Bonn *et al.*, Czech. J. Phys. **46**, 3195 (1996).
[38] The doping-dependent $\lambda(x)$ we deduce from the literature differs from that claimed by Uemura [Y. J. Uemura *et al.*, Phys. Rev. Lett. **66**, 2665 (1991)]. However, we find that even if we use Uemura's $\lambda(x)$ to extract J_{NL} or J_c, the doping trend of $J_{\mathrm{NL}}(x)$ remains essentially the same.
[39] A. Fuchs, W. Prusseit, P. Berberich, and H. Kinder, Phys. Rev. B **53**, R14 745 (1996).
[40] There are two reasons for choosing this temperature. First, the penetration depth diverges at T_c and its value near T_c is very sensitive to the choice of T_c. Therefore we would like to analyze our data at the lowest possible temperature. Second, the samples that are closer to the optimal doping level have a narrower $P_{3f}(T)$ peak and do not have strong P_{3f} signals below $0.97T_c$. To systematically analyze the doping dependence of the P_{3f} signals, $0.97T_c$ is the best compromise temperature.
[41] J. L. Luo, J. W. Loram, J. R. Cooper, and J. Tallon, Physica C **341–348**, 1837 (2000).
[42] Note the scale of $J_{\mathrm{NL}}(T=0.97T_c)$ and $J_c(T=0)$ from Luo *et al.* are quite different. This is because J_c drops rapidly near T_c. If we estimate $J_c(T=0.97T_c)$ from Luo *et al.* based on GL theory, the difference from J_{NL} is within one order of magnitude.
[43] V. J. Emery and S. A. Kivelson, Nature (London) **374**, 434 (1995).
[44] J. P. Sydow, M. Berninger, and R. A. Buhrman, IEEE Trans. Appl. Supercond. **9**, 2993 (1999).
[45] J. McDonald and J. R. Clem, Phys. Rev. B **56**, 14 723 (1997).
[46] M. Sigrist, Physica B **280**, 154 (2000).
[47] M. I. Salkola and J. R. Schrieffer, Phys. Rev. B **58**, R5952 (1998).
[48] G. M. Luke, Y. Fudamoto, K. M. Kojima, M. I. Larkin, J. Merrin, B. Nachumi, Y. J. Uemura, Y. Maeno, Z. Q. Mao, Y. Mori, H. Nakamura, and M. Sigrist, Nature (London) **394**, 558 (1998).
[49] M. Sigrist, D. B. Bailey, and R. B. Laughlin, Phys. Rev. Lett. **74**, 3249 (1995).
[50] F. Tafuri and J. R. Kirtley, Phys. Rev. B **62**, 13 934 (2000).